THE BEHAVIOUR OF REINFORCED CONCRETE SECTIONS UNDER BENDING, SHEAR AND TORSION

S. Sarkar*

Methods for the design and analysis based on some experimental and theoretical investigation into the behaviour of hollow rectangular reinforced concrete sections subjected to combined shear and torsion, and bending and torsion are discussed in this paper. In both parts of the investigation some intriguing results were observed which are reported here and explanations for these behaviours are put forward. For fuller details the readers are directed to three main references.

INTRODUCTION

The behaviour of reinforced concrete sections under combined loadings of (i) shear and torsion (under-reinforced) and (ii) bending and torsion (over-reinforced) is still not conclusively understood. Six under-reinforced rectangular R.C. sections were tested to failure under shear and torsion and eight over-reinforced sections under bending and torsion in order to observe their behaviour under load, to verify the validity of existing theories and attempt to develop bases of analysis for such sections. Some interesting phenomena observed during this study are reported in this paper with the hope that these may arouse some interest among readers to carry out further investigations in these areas.

* Professor and Head of Department of Civil Engineering, Surveying and Building, Dundee Institute of Technology, Dundee, Scotland

COMBINED SHEAR AND TORSION

Details of beams. Six 2.286 m long under-reinforced rectangular beams, three with 305 x 151 mm and three with 229 x 151 mm sections with a uniform wall thickness of 38 mm, were tested to failure primarily under shear and torsion. The deeper beams were reinforced with (a) longitudinal: 2-12.7 mm diameter and 1-9.5 mm diameter bars at bottom, and 2-9.5 diameter bars at top - these high strength bars had yield (proof) stress, f_y = 412 N/mm^2 and a modulus of elasticity, E = 206 kN/mm^2; and (b) transverse: Mild steel bars of 6.35 mm diameter (f_y = 309 N/mm^2) at 102 mm spacing for a length of 229 mm from the supports and then at 51 mm in the central portion of the beams, reinforcements. The shallower beams were reinforced identically to the deeper ones except that the bottom longitudinal reinforcement consisted of only 2-12.7 mm diameter high strength bars. The beams were tested with a longitudinal span of 1.829 m with the two transverse point loads being symmetrically applied at 0.457 m from the supports - this arrangement gave shear-span to depth ratios of 1.5 and 2.0 respectively for the deep and shallow beams. Torsion was applied at the ends of the beams by means of specially fabricated steel end brackets and loading arms - for details refer to Sarkar (1). The relevant details of the beams and the experimental results are given in Table 1.

Instrumentation, loading and control. The concrete strains on the surface of the beams were measured at 45° to the longitudinal axis of the beams at expected failure locations using 50 mm Demec extensometer giving a minimum strain reading of 0.5 x 10^{-5}. Electric resistance gauges were used to monitor strains in both longitudinal and transverse reinforcements. Simple mirror-telescope device was used for the measurement of the angle of twist with mirrors being attached to the vertical face of a beam, at mid-depth, at a gauge length of 1.219 m. The transverse loads were applied using hydraulic actuators and the torque using dead weights. The average of the properties of concrete for all the beams were as below:

f_{cu} = cube crushing strength = 34 N/mm^2
τ_{el} = torsional strength (elastic) = 3.4 N/mm^2
τ_{pl} = torsional strength (plastic) = 2.15 N/mm^2
E_c = elastic modulus = 23.4 kN/mm^2

EXPERIMENTAL AND THEORETICAL ANALYSIS

Shear and torsion. Table 1 gives an abstract of the

results of experiments and theoretical analysis for the beams tested under shear and torsion. The theoretical basis for the analysis is developed from the work by Lessig (2,3,4) and the main features are described here. Under the action of shear and torsion failure cracks at 45° to the longitudinal axis of the beam develop at the top, bottom and one vertical faces of the beam and the remaining vertical side provides a compression fulcrum - Fig 1. The shear stresses due to shear and torsion are additive on one vertical face and oppose each other on the other vertical face, Sarkar (5). For high ratios of shear to torsion pronounced formation of compression hinge, joining the extremities of failure cracks, was observed; for lower ratios the formation of compression hinge was not complete, but strain readings indicated development of compressive stresses. The other important factor observed was the smallness of the value of n, the depth of compression zone, given by $n = Q/(C_1 \times fc)$, and in most practical cases $n \leq 2b_2$.

Theoretical aspects. In the derivation of design/analysis formulae some simplifying assumptions are made, as given in a paper, Evans and Sarkar (6) viz, concrete in tension is fully excluded from work, the cross-section of transverse reinforcements is uniform in the failure zone, no local loads are present in the failure zone and all reinforcements intersecting the failure cracks reach yield point. The derivation is based on formation of equations of equilibrium for external and internal moments about two mutually perpendicular axes XX and YY (Fig 1). The moment due to external forces gives M_t', the 'equivalent torsional moment' due to the applied torque M_t and shear force Q and is given by:

$$M_t' = M_t + Q.\ (b - t)/2 \quad ..... \qquad (1)$$

In this equation the flexural moment is absent. The resisting moments are provided by the reinforcements intersecting the cracks. The moments due to horizontal and vertical legs of stirrups are given by

$$M_{th} = f_{yp}.\ A_{sp}.\ \frac{b_3}{s}\ d_3 \quad ..... \qquad (2)$$

$$M_{bh} = f_{yp}.\ A_{sp}.\ \frac{b_3}{s}\ (d + b) \quad ..... \qquad (3)$$

and

$$M_{tv} = f_{yp}.\ A_{sp}.\ \frac{d_3}{s}\ (b - b_s) \quad ..... \qquad (4)$$

and the total torsional resistance is given by

$$M_{th} + M_{tv} = f_{yp}.\ A_{sp}.\ \frac{d_3}{s}\ (2b_3 + b_s) \quad ... \qquad (5)$$

Then, for torsional moment equilibrium

$$f_{yp}\ A_{sp}\ .d_3\ .\ (2b_3 + b_s)/s = M_t' \quad \ldots\ldots \quad (6)$$

From eqn (6) the area and spacing of stirrups can easily be computed. The component M_{bh} gives a bending moment about XX axis and this moment must be resisted by longitudinal reinforcements which is preferably distributed uniformly over the vertical face. Assuming a total of A^h_{st} is needed this can be evaluated from:

$$A^h_{st} = \frac{f_{yp}.\ A_{sp}.\ b_3.\ (d + b)}{f_y\ .\ s\ .\ (b - b_2)} \quad \ldots\ldots \quad (7)$$

If A_{st} is the longitudinal reinforcement present at the bottom face of the beam then this amount has to be supplemented by an amount $A^h_{st}/2$ each at bottom and top corners of the failure crack on the vertical face of the beam.

Analysis of results. The forces, Q and M_t, at initial cracking (Table 1) were obtained by carefully monitoring the load increments, strain readings and surveying the faces of the beams for the development of cracks. Shear stress q is computed using $q = Q/(1.72\ td_1)$.

Torsional shear streses were computed for fully plastic and elastic distribution, τ_{pl} and τ_{el}. It was observed that the values of $(q + \tau_{el})$ were very close to τ_{el} of the control specimens, whereas, there was substantial variation, upto 20%, between $(q + \tau_{pl})$ and τ_{pl} of the control specimens. The actual (experimental) effective torsional moment M_t' was obtained by plotting M_t' vs strain in stirrups and picking up the value at yield of the reinforcement, Fig 2. The two forces Q_o and M_t at failure are given in columns 5 and 6 give the ratio of Q_o/Q_u, where Q_u, the ultimate shear strength of the beam, is obtained by using equation 8.

$$Q_u = 0.87.3.\ f_{yp}.\ A_{sp}\ (d_1 - n)/s \quad (8)$$

In order to relate Q_o and M_t column 9 was devised and the relationship is shown in Fig 3, where

$$\delta = M_t/[Q_o.\tfrac{1}{2}.\ (b - t)]$$

The experimental M_t' given by equation (1) and the corresponding theoretical M_t' obtained by using internal resistance of the section using equation (5) are given in columns 8 and 10 respectively. Finally, the tensile forces, F_1, in the longitudinal bars were computed and compared with those obtained experimentally as shown in columns 13 and 12.

Conclusions. There appears to be good agreement between the theoretical and experimental results. The shear strength of a section decreases with the increase in the proportion of torsional moments.

OVER REINFORCED BEAMS UNDER BENDING AND TORSION

Detail of beams. Eight over-reinforced hollow beams 152 mm x 194 mm deep with vertical and top wall thickness of 38 mm and bottom wall thickness of 45 mm were tested in this series (HB7 to HB14) for various $M_b/M_t = \phi$ ratios - Table 2. The properties of concrete were:

$f_{cu} = 30$ N/mm^2, $\tau_{pl} = 1.98$ N/mm^2, $\tau_{el} = 3.13$ N/mm^2 and

$E_c = 22.2$ kN/mm^2.

All the beams had 4-12.7 mm and 1-9.5 mm diameter bars (2.77%) as bottom reinforcements, and 6.35 mm diameter stirrups at 50 to 89 mm centres outside the test zone to prevent premature shear failure; HB/7, 8 and 9 had 2-9.5 mm, HB/11 and 13 2 - 12.7 mm, and HB/10, 12 and 14 2 - 15.9 mm diameter bars at top reinforcements. In the test zone, central 0.645 m, 6.35 mm diameter bars at 102 mm centres for HB/7, 8, 9 and 11, at 50.8 mm centres for HB/10, at 64 mm centres for HB/12, and at 127 mm centres for HB/13 and 14 were used. HB/7, 8, 9 and 11 were 3.708 m long (test span 3.251 m) and HB/10, 12, 13 and 14 were 2.286 m long (test span 1.829 m). Concrete strains were measured using a 100 mm Demec extensometer and steel strains using electric strain gauges. Non-linearity of concrete compressive strains was clearly observed even at low loads particularly with low $M_b/M_t = \phi$ ratios - a maximum compressive strain of 0.425% near failure of HB/14 was recorded.

Compressive zone. The depth of compression zone, n, was found by plotting longitudinal strain diagrams of all beams for both the vertical faces. From these plots a relationship between n and ϕ was obtained:

$$n/d = (0.56 - 0.75/\phi) \quad \ldots\ldots\ldots\ldots\ldots\ldots \quad (9)$$

Analysis of results. Ultimate limit slate method was used to obtain M_{bu}, and M_{tu} was computed using a method which takes into account the contribution of concrete, transverse and logitudinal reinforcements, Sarkar (1), as given in Columns 4 and 5 respectively of Table 2. M_{bu}, Column 8, was computed using n found from concrete

strain readings. It can be seen from column 9 that for beams HB/12 and HB/13 the experimental M_{bu} values are 23 and 30 percent greater respectively than the theoretical values. More interestingly it is further seen from column 10 that the corresponding experimental failure moments under combined loading are 18 and 26 percent greater than the pure flexural capacity of these beams. It is also seen from this column that there is a progressive decrease in flexural strength with decreasing value of ϕ with the exception of HB/12 and 13. Because of this apparent increase in strength for higher values of ϕ an attempt was made to compute f_c'', the strength of concrete, using the measured compression depth and the ratio f_c''/f_c' is shown in column 10, where f_c' is taken as $0.67\ f_{cu}$.

General behaviour of the beams. In all beams excepting HB/7 failure was accompanied by the crushing of concrete on the top face and the sides up to a depth n (Fig 5). It was noted that the inclination of the cracks to the longitudinal axis of the beams was much more acute than those for under-reinforced beams, Evans and Sarkar (6). Even in the case of HB/13 with ϕ = 10.4 this inclination was 70° at the soffit, which, for an under-reinforced beam would have been nearly 90°. Torque - twist and M_b Vs. mid-span deflection relationships were also studied. It was noted that for ϕ values up to 4 there was no marked increase in torsional stiffness of the beams over that of under-reinforced beams; however, significant increase in the torsional stiffness, upto 200%, was observed in beams tested for high values of ϕ. This may indicate that the longitudinal reinforcements may have little contribution towards increasing rotational stiffness, whereas, the contribution of concrete in the compression zone is quite significant. The beams subjected to low ϕ ratios exhibited loss of flexural stiffness, whereas, beam HB/13 showed approximately 20% increased flexural stiffness over beam HB/14.

Because of the apparent trend of an increase in the flexural strength capacity of the beams under combined load with high ϕ ratios a companion series of tests were carried out to study the strength of concrete under combined compression and torsional shear, reported in a paper by Sarkar (7), in which it was noted that concrete can exhibit an enhancement in compressive strength in the presence of small torsional shear stresses. Conversely it was also noted from column 12 that for low values of ϕ there appears to be slight increase in the torsional strength of the section.

Conclusions. (i) From the foregoing it is concluded

that for high values of ϕ there is a definite increase in the flexural strength of an over-reinforced R.C. beam, and referring to Fig 5 it may be seen that $\phi = 5$ appear to have some significance in that for $\phi > 5$ there is a tendency for the flexural strength to increase and the torsional strength to decrease. (ii) The straight line relationship given in equation (9) provides a basis for design of elements in combined bending and torsion when the criterion of failure is in flexural compression. (iii) An overall load factor of 2.0 is suggested for the design of members, and at this design moment the deflection should be less than 1/300th of span. The average angle of twist at this moment was found to be 4.7×10^{-6} radians/mm.

SYMBOLS USED

A_{sp}	=	area of one leg of stirrups (mm)
A_{st}, A'_{st}	=	area of bottom and top reinforcements (mm)
b , d	=	width and depth of beam (mm)
b_c,d_c	=	core dimensions of beams (mm)
d_1	=	effective depth of beam (mm)
b_2, d_2	=	cover to c.l. of longitudinal bars (mm)
b_s, d_s	=	cover to c.l. of stirrups
b_3	=	$(b - 2d_s)$: $d = (d - 2d_s)$
n	=	depth of compression zone
f_{yp},f_y	=	yield stress of stirrups and longitudinal bars
f_{cu}	=	cube crushing strength of concrete
ϕ		M_b/M_t ;
M_b	=	bending moment;
M_{bu}	=	failure bending moment in pure bending
M_t	=	torsional moment;
M_{tu}	=	failure torque;
Q	=	shear force;
Q_o	=	shear strength in combined shear and torsion
Q_u	=	ultimate shear strength
S	=	spacing of stirrups;
t	=	wall thickness

REFERENCES

(1) Sarkar, S. "Study of Combined Bending Torsion and Shear on Hollow R.C. Sections", Ph.D.thesis, University of Leeds, 1964.

(2) Lessig, N.N. "Determination of Load Carrying Capacity of Reinforced Concrete Elements with Rectangular Cross-section under Simultaneous Action of Flexure and Torsion", Beton i Zhelezobeton, No. 3, 1959, pp 109 - 113.

(3),(4) Lessig, N.N. "Study of Cases of Failure of Concrete in Reinforced Concrete Elements with Rectangular Cross-section subjected to Combined Flexure and Torsion", State Publishing Office of Literature on Structural Engg, "Design of R.C. Structures", edited by A.A. Gvozdev, Moscow, 1961, pp 311

(5) Sarkar, S. "Torsion on Reinforced Concrete Beams", Indian Concrete Journal, November 1959

(6) Evans, R.H., Sarkar, S. "A Method of Ultimate Strength Design of Reinforced Concrete Beams in Combined Bending and Torsion", The Structural Engineer, October 1965, No 10, Vol 43, pp 337-344.

(7) Sarkar, S. "The Behaviour and Failure of Plain Concrete Under the Action of Combined Compression and Torsion", Fracture of Concrete and Rock - Recent Developments, Elsevier Applied Science, 1989, pp 475 - 493.

TABLE 1 - Experimental and Theoretical Analysis of Beams in Shear and Torsion

	1		2			3	4	5	
Beam MK.	Initial cracking forces: Q(kN)	M_t(kNm)	Shear Stresses (N/mm) q	τ_{pl}	τ_{el}	$q+\tau_{pl}$ (N/mm²)	$q+\tau_{el}$ (N/mm²)	Forces at Failure Q_0 (kN)	M_t (kNm)
HB/1	22.24	2.07	1.17	0.88	1.08	2.05	2.25	362.5	5.42
HB/2	13.66	2.66	0.69	1.12	1.34	1.81	2.07	355.8	7.07
HB/3	8.45	2.66	0.43	1.12	1.34	1.54	1.81	347.8	7.47
HB/4	15.35	1.48	1.03	0.88	1.26	1.91	2.29	260.2	3.91
HB/5	10.01	2.07	0.68	1.22	1.76	1.89	2.44	201.5	4.02
HB/6	6.54	2.07	0.44	1.22	1.76	1.66	2.22	233.1	4.94

6	7	8	9	10	11	12	13
Qu (eqn 8)	Q_0/Q_u	M_t' (expt) (kNm)	$\delta=\frac{M_t}{Q_0\frac{(b-t)}{2}}$	M_t' (theor) (kNm) eqn 6	$\frac{M_t' \text{ (expt)}}{M_t' \text{ (theor)}}$	F_1 (expt) (kN)	F_1 (theor) (kN)
76.1	0.868	9.21	1.43	7.67	1.20	30.5	29.8
76.1	0.454	9.04	3.58	7.67	1.18	28.9	29.8
76.1	0.313	8.84	5.46	7.67	1.15	30.1	29.8
55.6	0.845	6.61	1.45	5.48	1.19	30.2	25.1
53.8	0.358	5.12	3.65	5.48	0.93	30.2	25.1
56.5	0.326	5.92	5.0	5.48	1.06	-	25.1

Beam dimensions: HB1, 2 & 3 - 151 mm x 305 mm
HB4, 5 & 6 - 151 mm x 229 mm

TABLE 2 - Over-reinforced beams - Experimental and Theoretical Results

	1	2	3	4	5	6	7	8
Beam MK.	$\frac{M_b}{M_t}=\phi$	Expt. Moments of failure (kNm) M_b	M_t	Computed ult moments (kNm) M_{bu}	M_{tu}	n (mm)	$\frac{n}{d}$	M_{bu}' computed from n (kNm)
HB/7	0	-	5.29	-	5.21	-	-	-
HB/8	2.0	10.96	5.48	25.12	5.21	31.8	0.185	12.20
HB/9	3.9	21.92	5.59	31.19	5.21	60.2	0.358	22.82
HB/10	3.9	26.32	6.77	40.22	8.34	95.3	0.51	-
HB/11	6.0	28.70	4.77	31.75	5.37	65.0	0.38	28.47
HB/12	5.7	37.28	6.48	31.75	8.83	74.4	0.426	30.28
HB/13	10.4	37.51	3.65	29.91	5.40	86.4	0.50	28.93
HB/14	-	37.96	-	37.28	-	95.3	0.56	37.28

9	10	11	12	13	14
$\frac{M_b \text{ (expt)}}{M_{bu}'}$	$\frac{M_b \text{ (expt)}}{M_{bu} \text{ (4)}}$	$\frac{fc''}{fc'}$	$\frac{M_t}{M_{tu}}$	Design Moments (load factor = 2.0) M_b	M_t
-	-	-	1.015		23.4
0.9	0.435	0.9	1.05	54	24.3
0.96	0.703	0.95	1.08	101	24.7
-	0.655	-	0.77	-	29.9
1.005	0.905	1.0	0.89	126	21.1
1.23	1.18	1.27	0.74	134	28.5
1.30	1.26	1.33	0.68	128	16.2
1.02	-	-	-	165	-

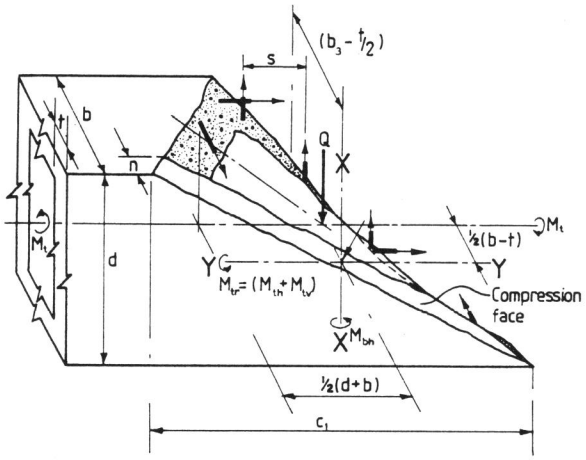

Fig 1 Mode of failure

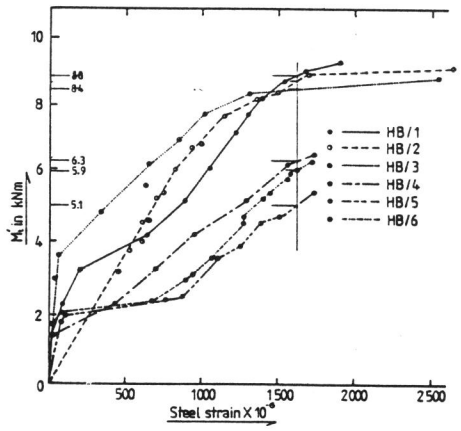

Fig 2 Relationship between M'_t and steel strain

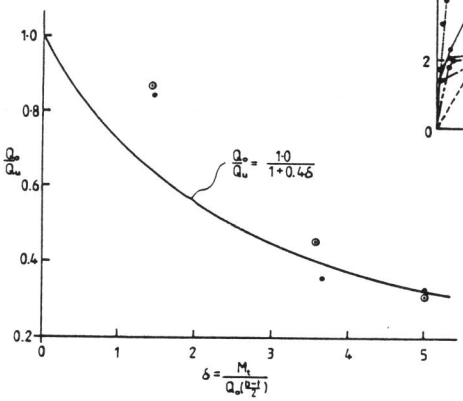

Fig 3 Relationship between Q_o/Q_u and δ

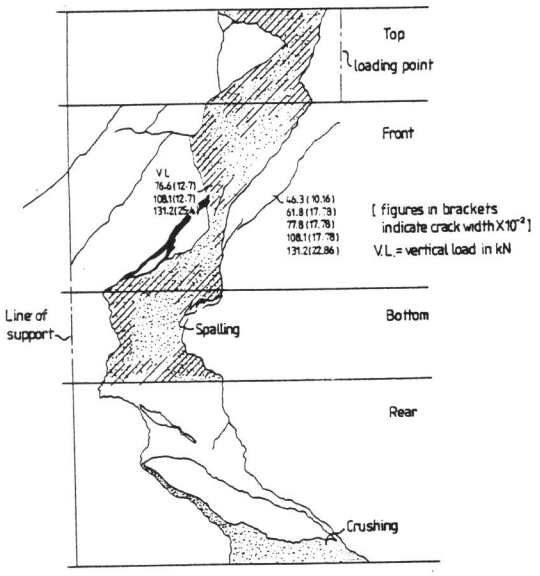

Fig 4 Exploded view at failure of HB/1

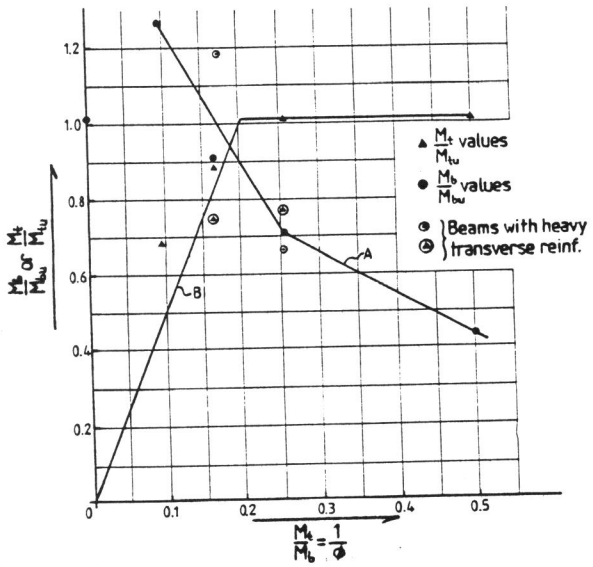

Fig 5 Relationship between M_b/M_{bu} or M_t/M_{tu} and $1/\phi$